

Noninvasive Detection of Early Therapeutic Response in Brain Tumors Using Functional Diffusion Mapping (fDM)

B. A. Moffat¹, C. Tsien¹, C. R. Meyer¹, A. Rehemtulla¹, T. L. Chenevert¹, B. D. Ross¹

¹Radiology, University of Michigan, Ann Arbor, MI, United States

Introduction: Diffusion MRI holds considerable promise for quantifying brain tumor response in rodents and humans. Changes in tumor water diffusion occur following successful treatment due to increases in the extracellular space, resulting from necrosis and/or apoptotic processes. Moreover, initial regions of necrosis and/or cysts may decrease in volume due to dynamic reorganization of the heterogeneous tumor structure following treatment. The change in cellularity due to cell kill pathways along with tissue reorganization may lead to heterogeneous changes in the underlying tissue morphology (e.g. ratio of intra- to extracellular water) resulting in spatially varying changes in tumor apparent diffusion coefficient (ADC) values. This heterogeneity in tumor ADC and change in ADC resulting from anti-neoplastic therapies means that traditional quantification of ADC such as mean ADC and change in mean ADC may not adequately describe the therapeutically induced changes in tumor ADC. This paper describes “functional diffusion mapping (fDM)”: a new method for quantifying heterogeneous changes in tumor morphology caused by anti-neoplastic therapeutic regimens. To demonstrate its utility we have evaluated fDM as an early therapeutic response predictor for primary brain tumors. In essence fDM is a statistical method that prospectively compares heterogeneous ADC maps acquired post-initiation of therapy with pre-treatment ADC maps where the two image data sets are co-registered and computationally analyzed to yield statistical maps of ADC change as color overlays on anatomical images (Fig’s: 1a-c) and scatter plots of ADC change (Fig’s: 1d-f).

Methods: Twenty patients presenting with unresectable primary brain tumors were recruited to participate in diffusion MRI studies to assess treatment response to fractionated chemotherapy, radiotherapy or radiochemotherapy. Radiographic treatment outcomes based on standard response criteria (1) was accomplished using the “crossed diameter product” (CDP) along with steroid use and were utilized to define clinical response classifications as follows: complete response (CR), partial response (PR), stable disease (SD), and progressive disease (PD). Written informed consent was obtained from all subjects, and all images and medical records were obtained according to protocols approved by the University of Michigan Medical School Institutional Review Board. ADC images were acquired on a 1.5T MRI system as previously described (2). MR images were spatially co-registered to the pre-treatment T₂-weighted images using a mutual information (MIAMI Fuse[®]) algorithm (3). For this study, tumor tissue was defined as that tissue which was either contrast enhanced on T₁-weighted images or for non-enhancing tumors, T₂ image hyper-intensity. ADC values of each voxel within the tumor ADC map at week 3 were plotted as a function of their pre-therapy ADC (Fig’s: 1d-f). All tumor voxels were then objectively segmented into 3 different categories: Red voxels (V_R) for which the ADC increased significantly (p<0.05); Blue voxels (V_B) for which the ADC decreased significantly (p<0.05); Green voxels (V_G) for which the ADC did not change significantly (p>0.05). The spatial distribution of these voxels was visualized by overlaying them (in color) onto the anatomical T₂ weighted MR images (Fig’s:1a-c). The total volume of the voxels within each category was calculated for each patient and normalized against the total tumor volume to give three normalized tumor volume segments V_R, V_B, and V_G.

Results: Figure 1 shows the fDM results from 3 patients with anaplastic oligodendrogliomas. Each patient received fractionated radiation therapy (70 Gy) and were subsequently classified as PD (Fig. 1a, d), SD (Fig. 1b, e) and PR (Fig. 1c, f). It was found that the V_R volumes of the PR patients were significantly (p<0.001) greater than those of the PD and SD patients (Fig. 2a). In addition the total volume (V_T = V_R + V_B) of responding tumor for PD patients were significantly (p<0.001) smaller than that of PR and SD patients (Fig. 2c).

Using a V_R threshold of 15%, fDM correctly identified all PR patients and distinguished them from SD and PD patients with a sensitivity of 100% (CI 61-100) and a specificity of 100% (CI 78-100). While a V_T threshold of 8% had a 100% sensitivity (CI 61-100) and specificity (CI 68-100) for discriminating between SD and PD patients.

Discussion: Early and accurate prediction of treatment response using alterations in MRI tumor diffusion values may provide an opportunity to switch to a more efficacious therapy in unresponsive patients thereby minimizing the morbidity associated with prolonged and ineffective treatment. Early modification of futile treatment regimens may also prove advantageous by reducing tumor resistance and provide for improved patient function thus enhancing clinical outcome in poor prognosis subgroups. Although the predictive values and overall accuracy were found to be 100 percent for all 20 patients based upon the quantitative fDM analysis, larger, prospective clinical trials will be needed to confirm these findings which could provide significant clinical and cost benefits. The fDM analysis presented here provides a simple visual display of regions that exhibit response and resistance to treatment, as well as offers the potential of a quantitative response grade via the scatter plot analysis.

References:

1. K. James, et al (1999). J Natl Cancer Inst. **91**, 523.
2. T.L. Chenevert et al (2000). J Natl Cancer Inst **92**, 2029.
3. C.R. Meyer et al (1997). Med Image Anal **1**, 195.

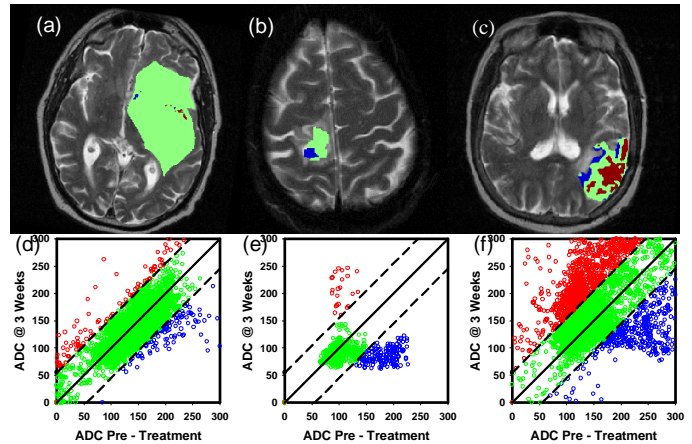


Figure 1. fDM maps and corresponding scatter plots of 3 gliomas with 3 different clinical outcomes.

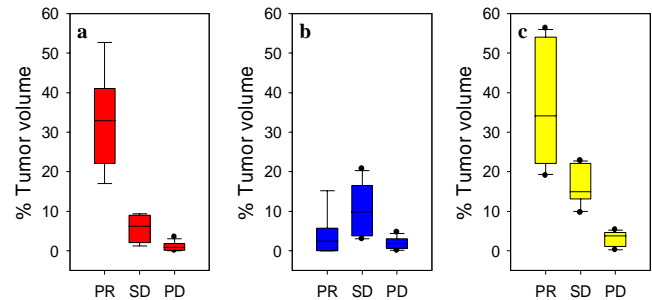


Figure 2: V_R(a), V_B(b) and V_T(c) results for the 3 response categories.

Acknowledgements:

This work was supported in part by the following NIH/NCI grants: P01CA85878, R24CA83099, P50CA01014.